Muhammad Awais
Sybille Krzywinski
Yordan Kyosev

Numerical Investigation of the Air Gap Distribution of Jackets with Different Fits and its Influence on Human Temperature

DOI: 10.5604/01.3001.0015.2727

TU Dresden,
Institute of Textile Machinery
and High-Performance Material Technology,
Germany

Abstract
The air gaps underneath clothing have a great influence on the thermal regulation of the human body. The distribution of the air gaps depends on the shape of the human body as well as on clothing style, fit, and deformation properties. This paper reports on the influence of clothing fit on thermophysiological parameters of the human body through thermal simulation. Four different fits of jacket and a test person were considered for the investigation and for simulation purposes. The results of the simulation concluded that different thermal regulations of the human body were exhibited for different fits of the jacket, which is due to distinct air gaps between the human body and clothing for each fit of the jacket. This research work presents a fast method to predict the influence of clothing fit on thermal comfort, which is usually studied by a time-consuming, laborious method – the wear trial.

Key words: *thermal simulation, 3D fit simulation of clothing, 3D scanning, air gaps, clothing fit, thermophysiological human model.*

Introduction

The human body tries to maintain its core body temperature at 37 °C by developing a thermal balance with the ambient environment [1]. Besides many other parameters; such as fabric characteristics, ambient environmental conditions, and the activity level of the human body, the clothing fit's impact on the microclimate also has a great influence on this thermal balance. Clothing fit objectively depends on the air gap between the overall 3D contour formed by the clothing and the 3D geometry of the human body [2]. The influence of clothing fit on the thermal regulation of the human body has long been reported by many scientists through experimental studies like subjective or objective wear trials. McCullough et al. [3] performed a series of wear trials on a standing thermal manikin for different fits of clothing. He reported that loose fit clothing has greater thermal insulation compared to tight fit clothing due to more air volume enclosed between the body and the textile. Havenith el al. performed a wear trial of loose and tight fit clothing with four different test persons in order to investigate the thermal insulation of the clothing during sitting and walking [4]. He concluded that during sitting, tight fit clothing had 6-31 % lesser thermal insulation compared to a loose fit, whereas during waking and the presence of wind the difference decreased. J. Fan also investigated the effect of clothing fit on the thermal and evaporative resistance of clothing [5]. He performed wear trials by means of a thermal manikin for fifteen jackets constructed from three different textile materials and with five different fits (S, M, L, XL, and XXL). He reported that both the thermal and evaporative resistance of the clothing increased with an increase in air gap, but after exceeding a certain value of the air gap, both resistances started to decrease, which was due to the start of the convection process in the air gaps, causing air movement and decreasing the thermal and evaporative resistance.

The new developments of 3D scanning tools and techniques have helped the scientists to analyse the distribution and quantification of the air gap volume more precisely [6-9]. Modern 3D scanning techniques allow analysis of the distribution of the air gap between the garment and the human body, as well as influence on it by the body shape, garment style and mechanical properties (drapability, bending rigidity) of fabrics [8, 10, 11]. The human body is movable and deformable, and it is not easy to be scanned with and without clothing in the exact same position. To overcome this difficulty, some scientists use 3D simulation for gap analysis [12-14]. The main advantages of this technique are that the draping of the clothing on the body are obtained at the time and that there is no need for the post-processing of scanning data. Research has demonstrated that the air gaps underneath clothing are not uniformly distributed. Actually, computations and analysis with non-uniform air gaps require the implementation of complex numerical methods which can

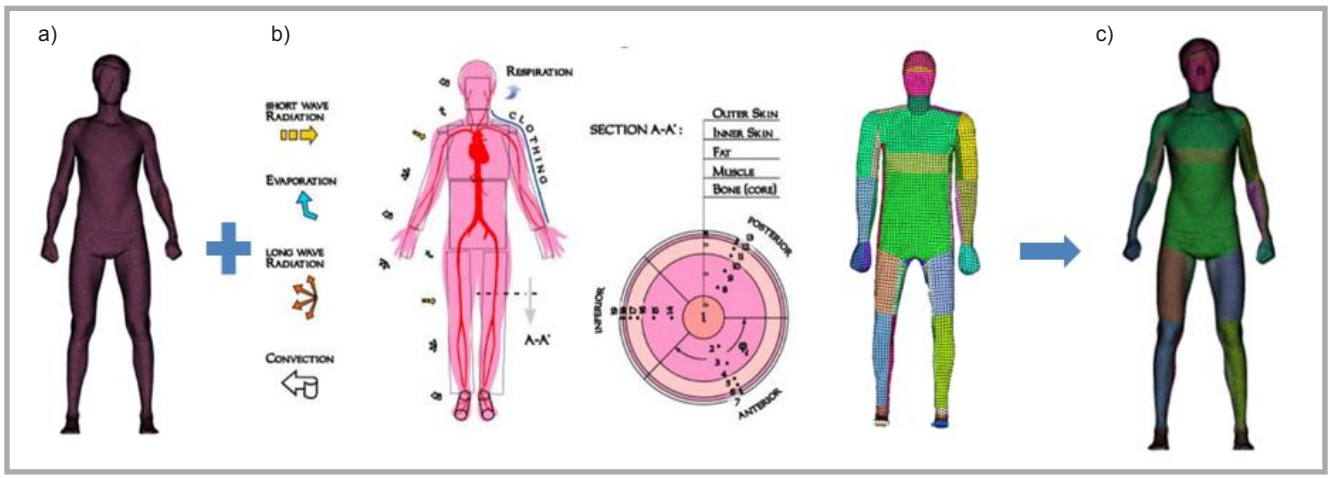

Figure 1. *a) Scanned data of the test person, b) the thermophysiological Fiala-FE model [35], and c) a thermophysiological model of the test person.*

consider the air motion and nonlinear geometries. In order to obtain a principal understanding of the influence of the air gap, many researchers have developed clothing models and thermal simulation methods with the assumption of a constant air gap thickness [15-18]. In recent years, advanced and reliable thermophysiological human models [19-23] and thermal sensation models [24-26] have been developed. Various researchers have already used these models and have proven their validity and reliability [27-33] and demonstrated that they can replace empirical investigations and can provide more accurate results compared to the models with a fixed air gap.

The focus of the present study was to prepare a computational model for the application of Theseus-FE and Fiala-FE software (integrated in the software) and conduct an analysis of the temperature distribution of the air gap developed within different fits of clothing. Study of the influence of different clothing fits on human thermophysiological parameters considering the human activity level was the other objective of the present research.

Finite element simulation with Theusus FE

Simulation of the heat transfer between the human body and clothing can be effectively performed using the software *Theseus-FE* [34]. This software has implemented the Fiala-FE model [35], based on the work of D. Fiala [36], which comprises a half-sphere for the head and solid cylinders for the remaining parts of the humanoid (***Figure 1.b***). The internal energy change within these cylinders and half-sphere is because of the radial conduction, arterial blood heating, and the metabolism, which is computed by the following partial differential ***Equation (1)*** [37, 38].

$$k\left(\frac{\partial^2 T}{\partial r^2}+\frac{\omega}{r}\frac{\partial T}{\partial r}\right)+q_m+ \\ +\rho_{bl}w_{bl}c_{bl}(T_{bl,a}-T)=\rho c\frac{\partial T}{\partial t} \quad (1)$$

where ρ is the specific mass of the body element (kg/m^3), c the specific heat of the body element (J/kgK), T the temperature of the body element (K), t the time (s), k the thermal conductivity (W/mK), r the body element radius (m), q_m the metabolic heat (W/m^2), ρ_{bl} the specific mass of blood (kg/m^3), w_{bl} the blood perfusion rate (m^3/s), c_{bl} the specific heat of blood (J/kgK), T_{bl} the arterial temperature (K), and ω is 1 for cylindrical body elements. ***Equation (1)*** explains the law of energy conservation for every layer of bodily matter e.g. skin, bone, muscle, fat, clothing etc.

The heat exchange between the environment and body surfaces due to convection, radiation, evaporation, and conduction on contact surfaces can be realised in Theseus-FE by defining the boundary conditions. Both types of convection; natural and forced, can be defined by using the combined convection coefficients (***Equation (2)***).

$$Q_{conv}=A_{sf}h_{c,mix}(T_a-T_{sf}) \quad (2)$$

Here, Q_{conv} is the convective heat flux (W), A_{sf} the body surface area (m^2), $h_{c,mix}$ the combined convection coefficients (W/m^{2}K), T_a the ambient air temperature (K), and T_{sf} the surface temperature (K). For computing the combined convection coefficient, D. Fiala used the validated function from ***Equation (3)***, where $V_{air,eff}$ is the effective airspeed (m/s) and $a_{nat,j}$, $a_{frc,j}$ & $a_{mix,}$ are the coefficients which are defined in ***Table 2*** in [19].

$$h_{c,mix}= \\ \sqrt{a_{nat}\sqrt{|T_a-T_{sf}|}++a_{frc}V_{a,eff}+a_{mix}} \quad (3)$$

The radiative heat transfer (Q_{rad}) in *Theseus-FE* is derived from the shell-model and then applied to the internal manikin model (***Equations (4)*** and ***(5)***). Radiative phenomena like the view-factor, radiation heat from the sun, and transmission (e.g. glass) can be considered in Theseus-FE.

$$Q_{rad}=A_{sf}h_r(T_w-T_{sf}) \quad (4)$$

$$h_r=\sigma\varepsilon_{sf}\psi_{sf-w}({T_w}^2+{T_{sf}}^2)(T_w+T_{sf}) \quad (5)$$

where T_w is the wall temperature (K), h_r the radiative heat transfer coefficient (W/m^{2}K), σ the Stefan Boltzmann coefficient (Wm^{-2}K^{-4}), ε_{sf} the body surface emission coefficients, and $\psi_{sf\text{-}w}$ is the view factors. The same coefficient values of body surface-emission were used by *Theseus-FE*, which was defined by D. Fiala for each body element according to its location and temperature [20, 38].

The evaporative heat loss ($Q_{e,cl}$) from the skin is realised through the partial pressure difference between the skin and ambient air (***Equation (6)***) [38].

$$Q_{e,cl}=A_{sk}U_{e,cl}(p_{sk}-p_a) \quad (6)$$

Where p_{sk} is the water vapor pressure at the skin (Pa), p_a the water vapor pressure of

air (Pa), and $U_{e,cl}$ is the resultant evaporative heat transfer coefficient ($Wm^{-2}Pa^{-1}$), explained in [20, 38]. The sum of heat fluxes Σq_{bc} due to convection, radiation, contact, and evaporation is integrated on the skin/clothing layer of the model and builds the thermal load *F(T)*.

$$q_i^e = A\phi_i^e \sum q_{bc} \text{ for } \xi = 1 \qquad (7)$$

The complete body geometry is discretised to elements, which equations together with the boundary conditions build a complete matrix system, as explained in [38].

$$M(T)\dot{T} + K(T)T = F(T) \qquad (8)$$

Here, *T* is the temperature matrix, Q the heat flux, *M* the capacity matrix, *K* the conductivity matrix, and *F* is the thermal load vector, all depending on the temperature *T*.

Equation (8) contains the first derivative of the temperature field, and it has to be solved for the transient case through time. For this, the temperature field in the next time step is solved with Theseus-FE software using the backward Euler method.

The thermal load *F(T)* includes the metabolic heat of the human body, which depends on the weight and activity of the motion, and is calculated by using the following relation [39]:

$$ME = 1.5W + 2.0(W + L)\left(\frac{L}{W}\right)^2 + \\ + \eta(W + L)(1.5v^2 + 0.35vG) \qquad (9)$$

where *ME* is the metabolic rate (watt), *W* the body weight (kg), *L* the carried load (kg), *v* the walking speed (m/s^2), η the nature of the terrain, and *G* is the walking grade.

The complete workflow for the solver is visualised in ***Figure 1***. The scanned human surface (***Figure 1.a***) in the form of triangulated mesh is coupled with the Fiala-FE model (***Figure 1.b***), which provides information about heat transfer at different states of the body according to the Fiala Model. This information is distributed into several zones over the surface mesh (***Figure 1.c***), and this mesh is used in *Theseus-FE* for the solution of the bioheat equation. The software allows the selection of a different number of zones of the human surface, specifying their exact parameters, where the influence of the air gaps on the thermal behaviour of the body is integrated.

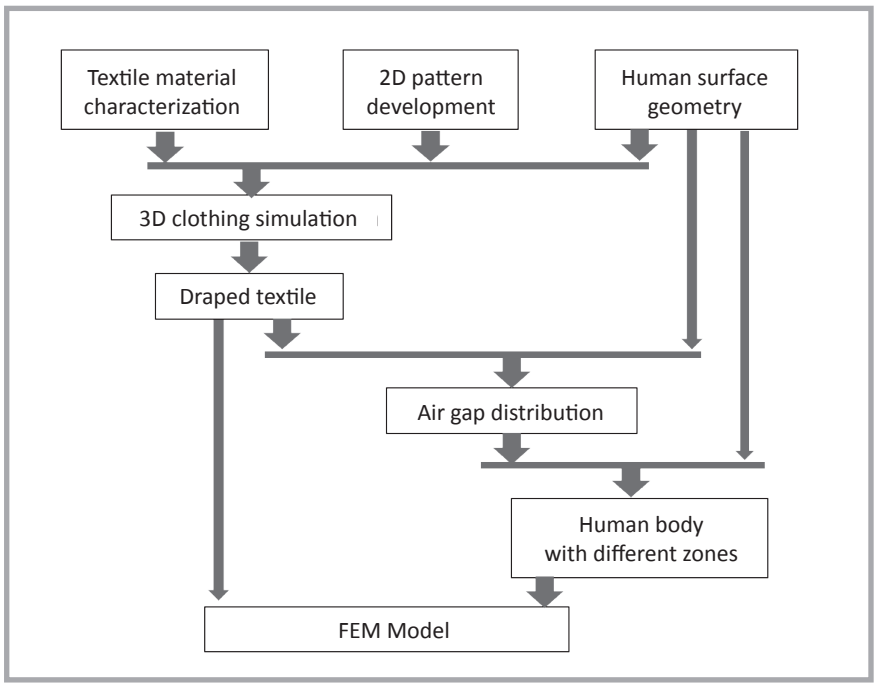

Figure 2. *Data flow of FEM model preparation.*

Table 1. *Characterisation of material.*

Characteristics			Values	Instruments	Standard
Physical	Fabric thickness [mm]		1.55	Karl Schröder KG Material Testing Machine	DIN EN ISO 5084
	Average mass per unit area of the fabrics [g m^{-2}]		168	GSM Cutter, weighing balance	DIN EN 12127
Thermal	Water vapour resistance [m^2 Pa W^1]		5.57	Sweat guarded hot plate	DIN ISO 11092:2014
	Thermal resistance [m^2 K W^{-1}]		0.063	Sweat guarded hot plate	
	Specific heat [$Jkg^{-1}K^{-1}$]		1640	Calculated	Calculated
Mechanical	Bending stiffness [μN m] (warp, weft, 45°)		2.87, 2.88, 2.91	Bending stiffness tester Cantilever ACPM 200	DIN EN ISO 9073-7
	Elongation [%] at a specific force			Zwick Tensile Strength Tester	DIN 53835
	Force 5 N/m	Warp	0.42		
		Weft	1.27		
	Force 20 N/m	Warp	2.00		
		Weft	6.4		
	Force 100 N/m	Warp	7.17		
		Weft	28.20		
	Spring stiffness [N/m] in the diagonal direction for consideration of the shear in the 3D simulation		57.48		Calculated, based on elongation at 5 N/m in the diagonal direction G=123/EB5

Table 2. *Alteration in ease allowance for developing jackets of different fits.*

Measurements	Ease allowances			
	Normal fit, cm	Tight fit, cm	Loose fit, cm	Extra loose fit, cm
Chest circumference	6.50	1.00	11.50	14.50
Shoulder length	1.00	0.75	1.50	1.75
Arm hole depth	5.00	3.00	5.00	7.00
Addition back arm hole	1.00	0.50	1.25	1.40
Reduction front arm hole	1.00	1.50	1.75	0.60
Cuff circumference	10.00	8.00	12.00	14.00

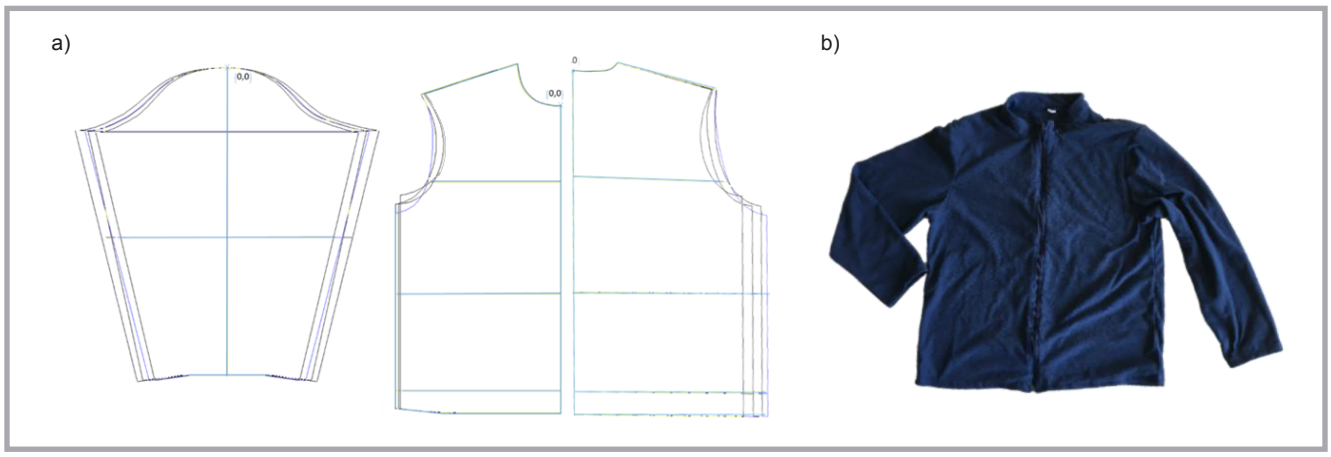

Figure 3. *a) 2D patterns for jackets of different fits (tight, normal, loose, and extra loose), b) normal jacket fit*

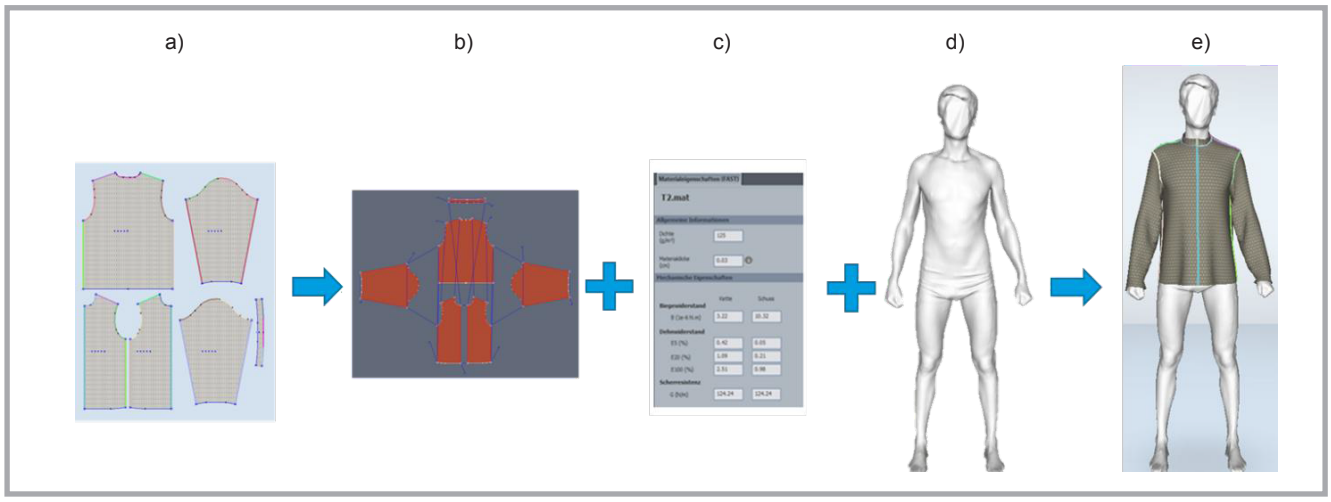

Figure 4. *Process chain of 3D fit simulation (defining of seams, assigning material properties, positionng of pattern cuts, and simulation).*

Preparation of the computational model

The preparation of data for the simulation consists of several steps, represented in ***Figure 2*** and discussed in detail in this section. In these steps, the scanned 3D human geometry was used several times – once together with the 2D pattern and the textile material parameters as a basis for the draping simulation; the second time – to calculate the distance between the human geometry and clothing for air gap distribution, and finally – the third time as a basis for the FEM model. The final FEM model consists of two sets of shell elements – those of the clothing and human body.

The jackets investigated consist of weft knitted fabric made of 100% polyester, with additional mechanical finishing in order to get the fleece side for higher temperature insulation. Characterisation of the material was made according to the requirements of fit and thermal simulation. ***Table 1*** shows the physical, mechanical, and thermal properties that were measured and calculated.

A volunteer test person aged 26 years of 85 kg weight and height of 197 cm was selected for performing the thermal simulation. The 3D surface of the test person was obtained by scanning the standard normal standing position with the help of Vitus XXL 3D body scanner [40]. The point cloud data were then processed by *Geomagic Studio* software [41], where the scan data were cleaned, refined, and prepared for further simulation processes as a NURBS (Non-uniform rational B-splines) model.

A clothing model of a jacket with a normal fit, shown in ***Figure 3.b***, was selected for the present research work, and then later further three fits of the jacket – tight, loose, and extra loose fit were derived from the 2D cut pattern of the normal fit.

The estimated body measurements according to ISO 8559 for the normal fit were imported into *Grafis* software [42], which was used to construct 2D cut patterns of the jacket. *Grafis* keeps the construction of the pattern based on a size-dependent formula (z-value) and ease allowance (x-values) and allows automatic grading of the pattern to other fits by changing the ease allowance (x-values). ***Table 2*** shows ease allowances for different measurements that were changed to derive different fits of jackets.

The 2D cut patterns were exported from *Grafis* as an AAMA/DXF file for use in the next step – 3D fit simulation with *Modaris V8* software [43]. Modaris V8 was selected because it provides one exactly described procedure for determination of the material parameters, which then can be determined using standard testing devices. This was an important prerequirement for proper physical simulation at the time of the beginning of this

study. Today some more software packages can be applied and a comparison between them can be performed, but such a study is subject to future investigations. After the importing of the 2D patterns (***Figure 4.a***), the sewing lines were defined according to the design (***Figure 4.b***). The material parameters were tested according to DIN 53835 and the required values were calculated in the Modaris Menu of the FAST (Fabric Assurance by Simple Testing Systems) system. The values required according to FAST for the force at 5%, 20% and 100% elongation were taken from the force-elongation curve. The shear resistance was calculated based on elongation EB5 at 5 N/m in a bias-extension test following the recommended equation G = 123/EB5.

Finally, the imported scanned mesh of the testing person was virtually dressed with the jacket, where the equilibrium conditions for the contact forces, material parameters, and clothing geometry were considered with the Modaris draping simulation algorithms implemented in. They are not publicly available, but principally they are known as mass-spring systems; an explicit integration was used for solving such problems. This procedure was repeated for each fit of the jacket for the test person, the results of which are demonstrated in ***Figure 5***.

In the present scenario, it can be noticed in ***Figure 5*** that the draping behaviour of every fit of the jacket is different than for the others and, therefore, resulted in different air gap development in each case of fit of the jacket. Therefore, air gap size analysis was carried out with the help of *Geomagic Qualify* software for each fit of the jacket, as shown in ***Figure 6***. This analysis confirmed some previous investigations and the author's expectations that air gaps are not distributed uniformly all over the body.

The models of jacket and test person were imported into Theseus-FE software as a mesh of shell elements consisting of 53919 and 44349 triangles, respectively (***Figure 7***) The large number of elements is based on the complexity of the human and textile surface as well as the need to cover this geometry with enough good mesh, which leads to an element size of a few milimeters. The preliminary tests showed that at such a mesh size the errors from the numerical computations were already significantly smaller than

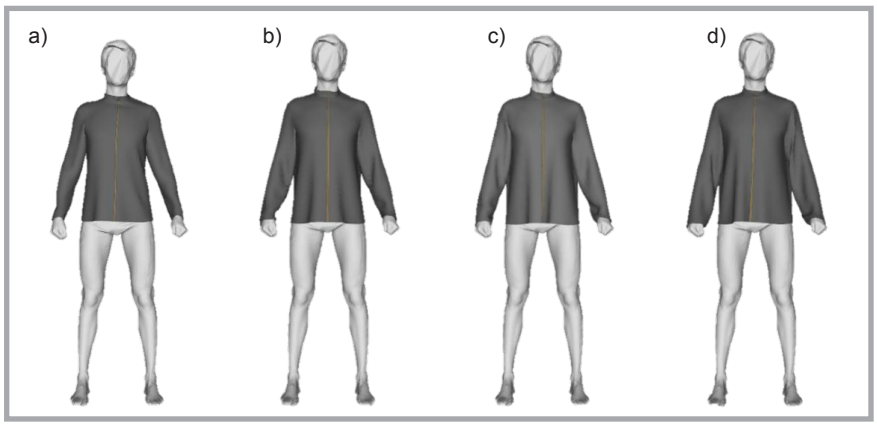

Figure 5. *Fit simulation of the jacket: a) tight, b) normal, c) loose and d) extra loose for test person.*

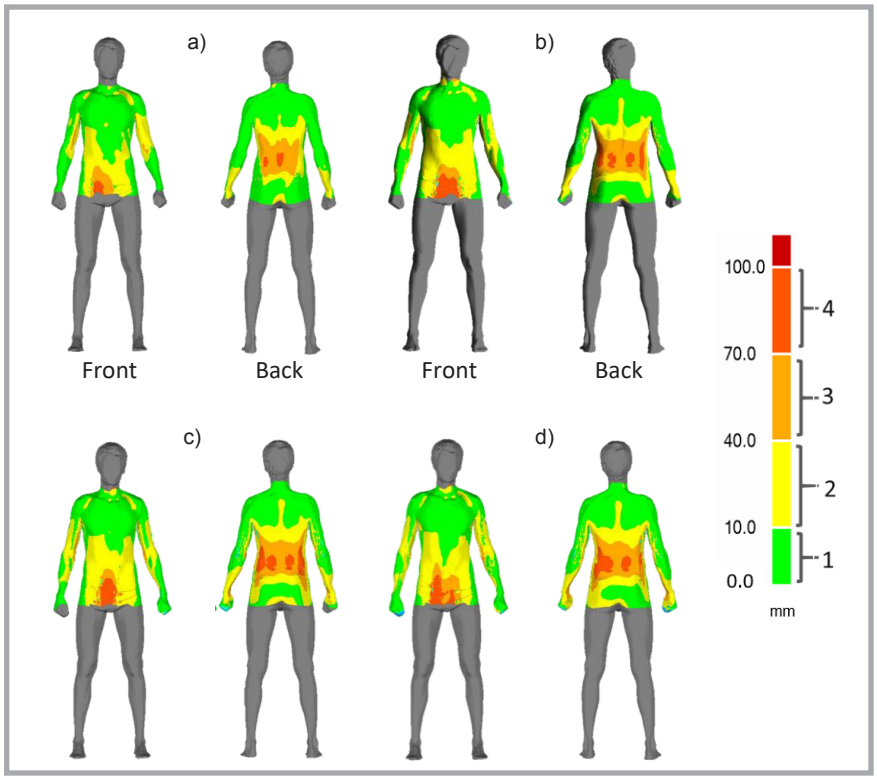

Figure 6. *Air gap size of all fits of jacket: a) tight, b) normal, c) loose, and d) extra loose, visualised over the human body surface (not over the jacket).*

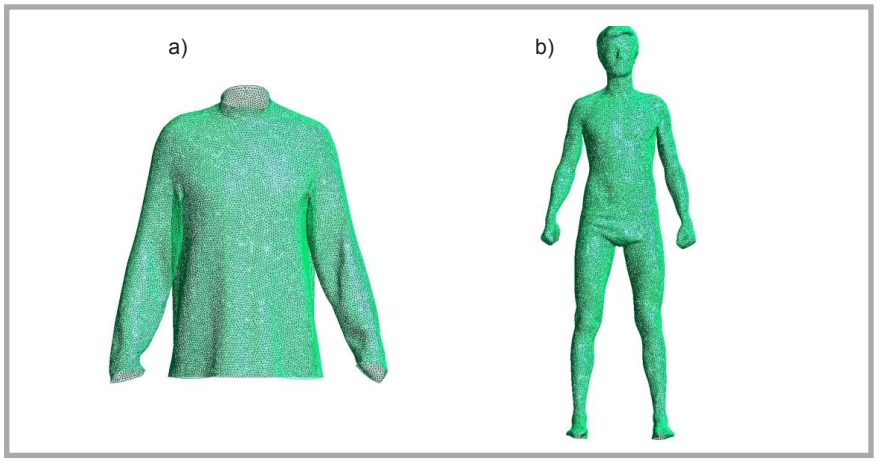

Figure 7. *FEM Models of a) the jacket and b) the test person.*

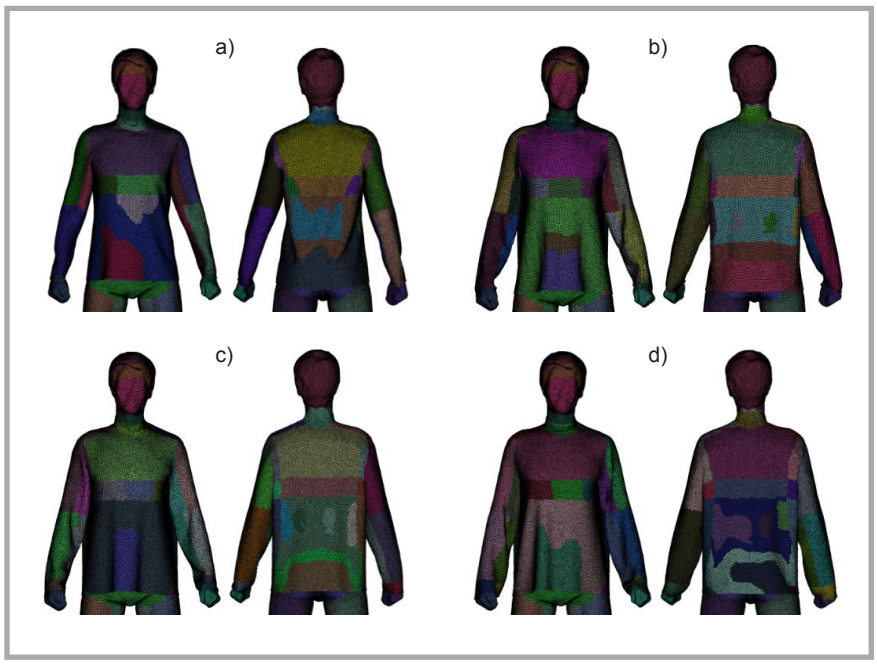

Figure 8. *The different colours show the different air zones for a) a tight fit jacket, b) a normal fit jacket, c) a loose fit jacket and d) an extra loose fit jacket.*

Table 3. *Metabolic rates of test person for different activity levels.*

Phase	Activity	Duration, min	Metabolic rate	
			Watt	MET
1	Sitting (0 km/h)	15	124.8	1.2
2	Walking (4 km/h)	40	270.4	2.6
3	Sitting (0 km/h)	15	124.8	1.2
4	Walking (6 km/h)	40	436.8	4.2
5	Sitting (0 km/h)	15	124.8	1.2

the remaining errors of the model built, like material parameter determination, gap size, and metabolism parameters. For this reason, additional simulations with a finer mesh size were not performed. The air gap distributions calculated were used for the definitions of the different zones over the human body in dependence on the air gap size and their location on the body segment (***Figure 8***). In ***Figure 8***, the different colours on the surface of the jackets represent the air zones with different heat transfer coefficients. For this purpose, it was considered that every air zone was a rectangular cavity in which free convection took place. The heat transfer coefficient of each air zone (assumed as a vertical-cavity) was calculated with the help of the Nusselt number, which is the function of the Prandtl and Rayleigh numbers [44] The processes of coupling the Fiala-FE model with the scanned data of the test person, dividing the air gaps into air zones, and calculating the heat transfer coefficient were investigated comprehensively in [32, 33]

In the current case, the transient simulation was performed to see the development of the temperature with respect to time. Furthermore, before running the thermal simulation, all the boundary conditions required for the thermal simulations were defined for the model:

- All the thermal and physical properties, like specific heat, conductivity, thickness, and mass per unit area were defined for the jacket surface.
- An environment was defined with an air velocity of 0.3 m/sec; the environment temperature was set at 23 °C and 50% relative humidity.
- The heat transfer due to longwave radiation was realised by defining the view factor cavity, and radiation properties of the test person and clothing.
- Heat transfer among the air gaps, clothing surface, and body surface was realised with the help of the heat transfer coefficient, which was calculated for every air zone.

For the simulation, the activity of the human was separated into five phases, where periods of sitting and walking were alternated, following ***Table 3***. The metabolic rate in ***Equation (9)*** was computed for a human without additional weight and running in stable terrain (treadmill) Thus, the values of L and η in ***Equation (9)*** were taken as 0 and 1, respectively.

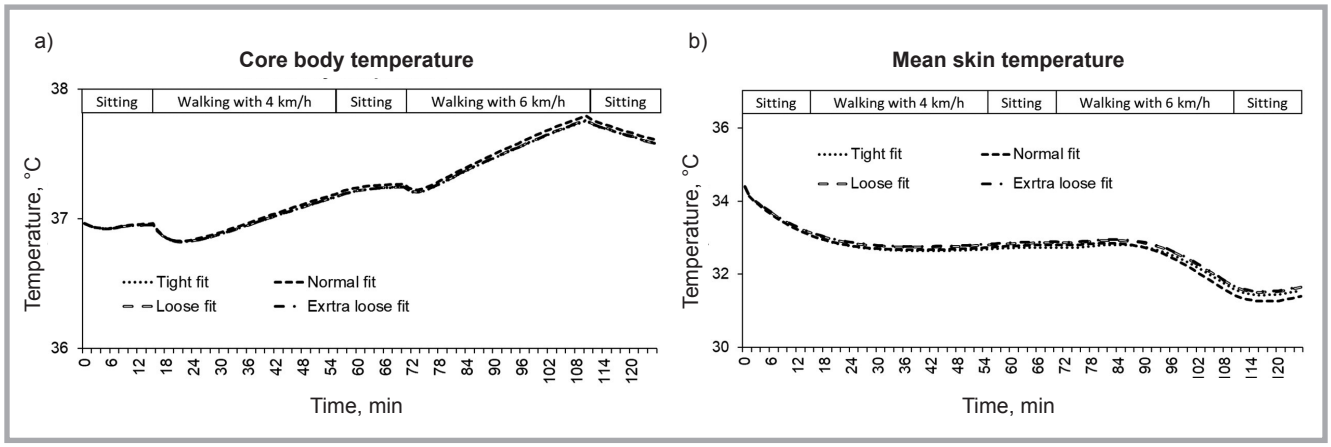

Figure 9. *Core body temperature a) and mean skin temperature b) during the thermal simulation of TP-1 with different fits of jacket.*

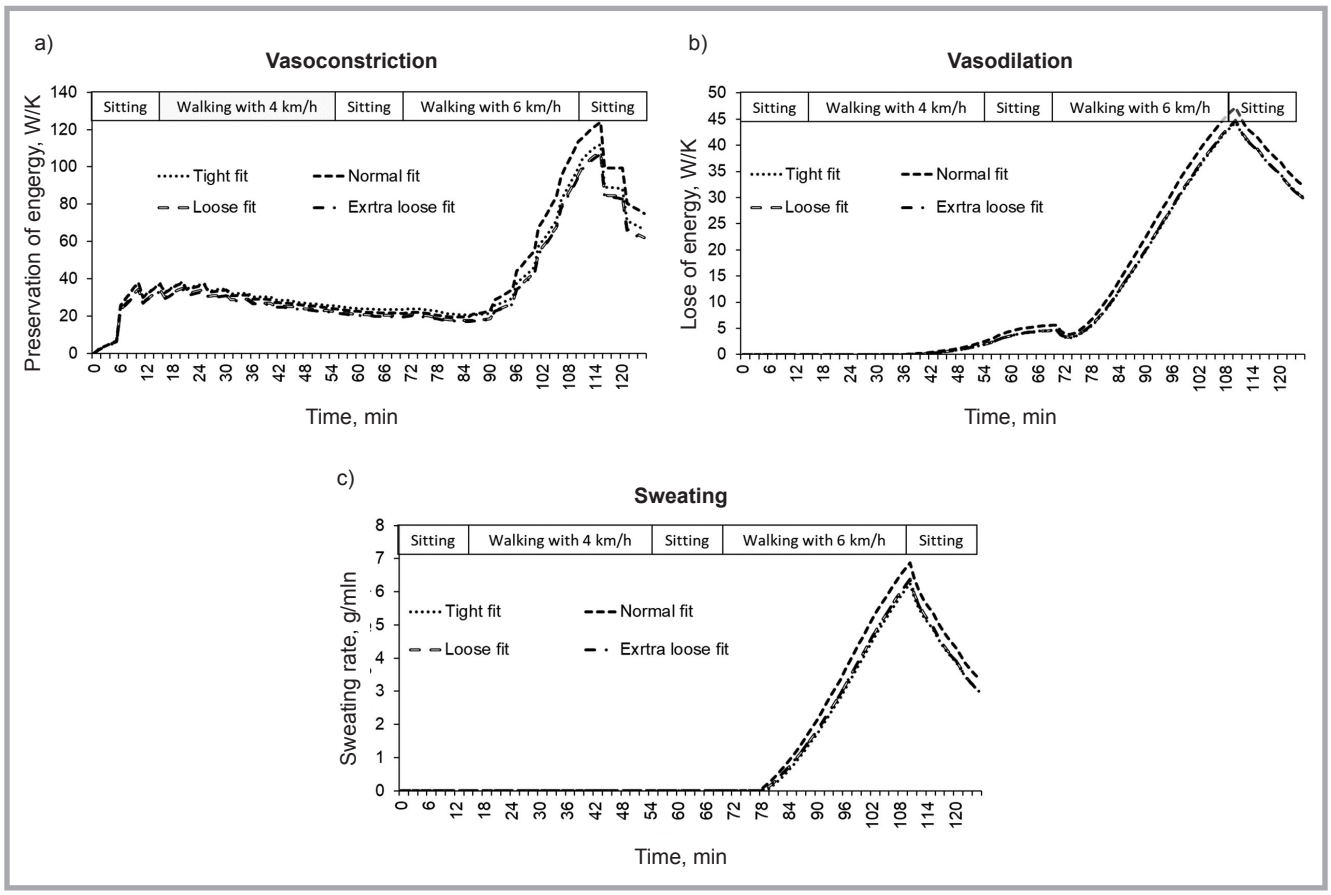

Figure 10. *Responses of the active system of TP-1 for CS-III: a) vasoconstriction, b) vasodilation and (c) sweating.*

Numerical results and discussion

Figure 9 shows the thermophysiological responses of the test person in terms of the core body and mean skin temperatures during the thermal simulations of jackets with different fits. It can be noticed in ***Figure 9.a*** that there are not many fluctuations in core body temperatures during sitting phases. However, during the 2nd and 4th phases, the core body temperatures increase significantly, due to the rise in metabolic rates, which increased during walking at 4 km/h and 6 km/h in the 2nd and 4th phases respectively. Furthermore, the core body temperature of the test person in the case of a normal fit jacket is little bit higher compared to the other fits of jacket (more visible in the 4th phase). Whereas the core body temperatures of the test person in the case of the loose fit and extra loose fit show the lowest values. It can be concluded that the normal fit jacket offers higher thermal resistance than the loose and extra loose fits. The reason for the lower thermal insulation of the loose and extra loose fit jackets are the folds that are produced on the surfaces of the jackets during draping on the body. It is already experimentally proven that the folds in garments cause more heat loss from the body as compared to homogeneous air gaps [45]. As the air gaps in the case of normal and tight fits of jacket are more homogeneous, they prevent loss of heat of the body. Furthermore, it can also be noted from ***Figure 9*** that the tight fit jacket does not present as much of a thermal load as does the normal fit; even a normal fit has more folds on the jacket surface compared to the tight fit, which is due to the optimum air gap thicknesses causing maximum thermal resistance in the case of the normal fit.

In comparison to the core body temperature, the mean skin temperatures of the test person start to decrease with the start of the simulation (***Figure 9.b***). This is due to the heat flow from a higher temperature surface (skin temperature – 35 °C) to a lower temperature (environmental temperature 23 °C). With the start of the 2nd phase, the mean skin temperatures stop falling due to the higher metabolic rate producing more heat in the body. Subsequently, vasoconstriction also stops increasing, which started as the result of a sudden fall in the mean skin temperature in the 1st phase (***Figure 10.a***). Furthermore, the mean skin temperatures of the test person remain the same in the case of all the jackets until the middle of the 4th phase (6 km/h). Then a sudden fall can be seen in the mean skin temperatures, which is because of the sweating. The activation of sweating and vasodilation in the 4th phase (as shown in ***Figures 10.b*** and ***10.c***) is the result of an increase in the core body temperature (***Figure 9.a***), which must be maintained at 37 °C by releasing heat to the environment. On the other hand, a sudden increase can be seen in vasoconstriction (***Figure 10.a***), which is the result of a decrease in the mean skin temperature. Hence, this complex scenario of the heat regulation of the body is controlled by the combined working of three processes of the active system: vasodilation, vasoconstriction, and sweating, to maintain the body's temperature at set points.

It can also be seen in ***Figure 10*** that the normal fit causes more extreme responses of vasoconstriction, vasodilation, and sweating compared to the other fits of jacket. As the normal fit jacket develops

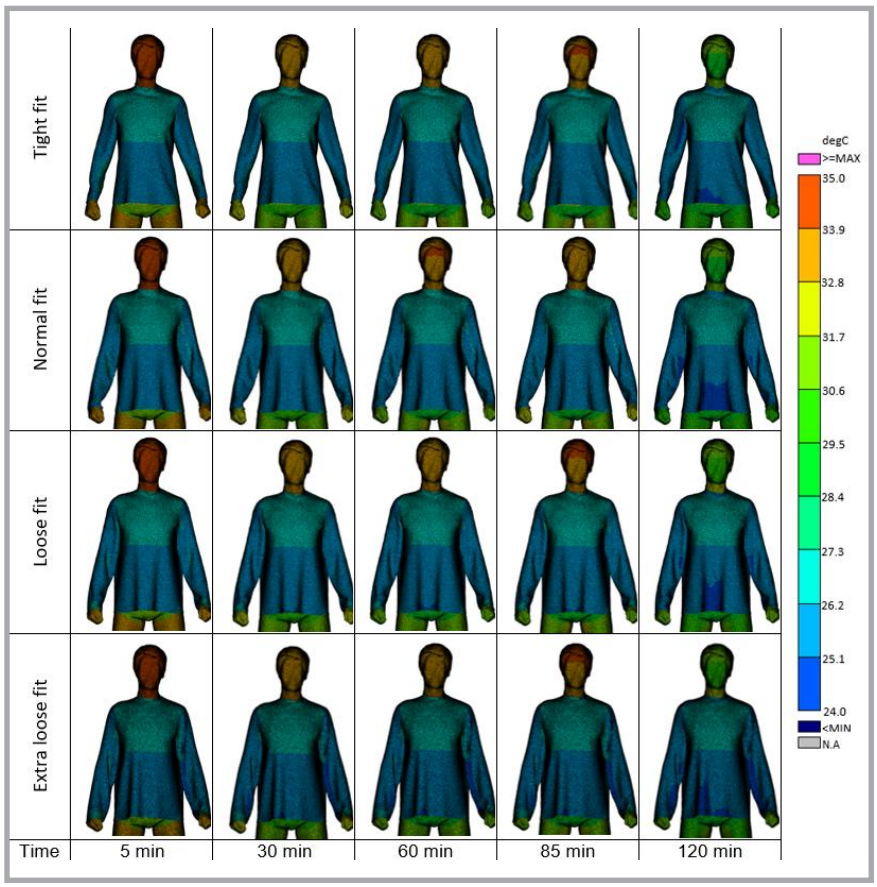

Figure 11. *Surface temperature of the clothing at different time steps during thermal simulation.*

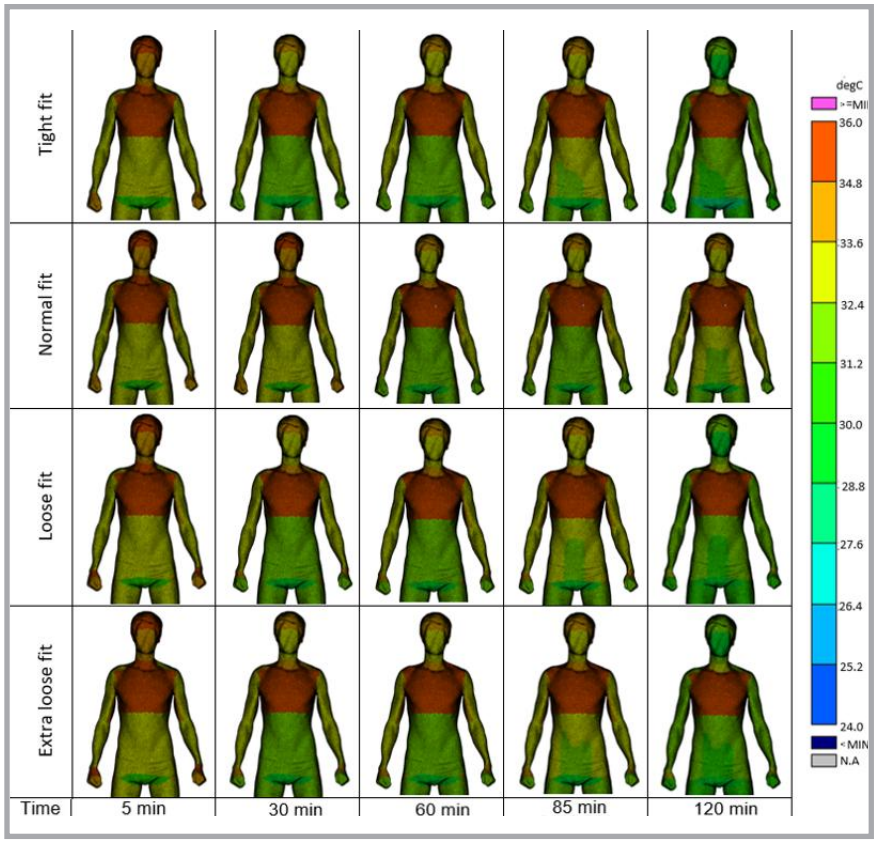

Figure 12. *Local skin temperature of the TP-1 at different time steps during thermal simulation.*

more thermal load (core body temperature is higher compared to the other fits of jacket; ***Figure 9.a***) due to higher thermal resistance, the values of vasodilation and sweating are higher compared to the other fits of jacket in order to release heat from the body, see ***Figures 10.b*** and ***10.c***). Moreover, more production of sweating becomes the reason for a more cooling effect on the skin; therefore, a lower mean skin temperature can be noticed in the case of the normal fit. Since the activation of vasoconstriction relates to lower skin temperature, a higher value of vasoconstriction in the case of the normal fit jacket can be observed.

A visual presentation of the jacket's surface, local skin and microclimate temperatures at different time steps during the thermal simulation of the jackets and test person can be seen in ***Figure 11***, ***Figure 12***, and ***Figure 13***, respectively.

The variation in the surface temperature of the jackets increases with an increase in the loose fit, i.e. the extra loose and loose fit jackets have more surface temperature variation. This is due to the folds in the jackets, which produce air gaps of more uneven width, see ***Figure 11***. Consequently, minimum temperature variations can be seen on the smoother surface of the tight fit jacket. Moreover, the jacket surfaces at the chest show almost the same temperature, which is due to the smooth and same draping behaviour of the fabric at the chest. However, the jacket's draping behavior in the abdomen area of the body is not smooth and differs in each fit of jacket.

As the air gaps at the chest are almost the same in each case of the jacket, the chest skin temperatures also have the same values, and the lower part of the body (abdomen) shows significant variations in skin temperatures, see ***Figure 12***. It is evident that the draping behaviour and air gaps have an influence on skin temperatures. The same effects of the air gaps on the microclimate temperature can be noticed in ***Figure 13***. The temperature behaviour of the air gaps belonging to the chest show almost the same values, whereas there are considerable variations in the temperatures of air gaps at the lower part of the body (abdomen).

It can be concluded from the simulation results of jackets that the normal fit has the optimum thermal resistance compared to the other fits of jacket.

In other words, the ease allowances (chest circumference: 6.50 cm, armhole depth: 5.00 cm, and cuff circumference: 10.00 cm – see ***Table 2***) that were given to the normal fit jacket produced air gaps of maximum thermal resistance in the scenario presented. Furthermore, it can also be concluded that air gaps considerably influenced the thermal resistance of the clothing system, which can be managed by adding and removing the ease allowances of the clothing.

Conclusions

In the present study, a computer-based thermal simulation method was used to analyse the influence of clothing fit on the thermophysiological parameters of the human body. The method consists of the scanning of the test person, development of a thermophysiological model of the test person, 3D fit simulation of four different fits (tight fit, normal fit, loose fit, extra loose fit) of the jacket, air gap thickness (between clothing and the human body) analysis, and thermal simulation taking into account the metabolic rate. The non-uniform layer of air underneath the clothing was considered, and heat transfer coefficients of different thicknesses of the air gap were calculated, which were used during thermal simulation. It has been concluded from the results that clothing fit has a great influence on the thermophysiological parameters of the human body, microclimate, and clothing surface temperatures. Furthermore, the differences in local skin temperatures increase with an increase in loose and extra fits, which is due to the folds in the fabric being more visible, especially in the abdomen area of the body. On the other hand, all fits of jacket have the same smooth draping behaviour at the chest, which results in almost the same jacket surface and skin temperatures. It is also noted that the normal fit of jacket causes more thermal load (higher core body temperature) and sweating compared to the other fits, from which it can be concluded that in the present scenario the normal fit jacket provides more thermal resistance compared to the other fits. Whilst the extra-loose fit provides the minimum thermal resistance, thus causing a lower thermal load compared to the other fits of jacket.

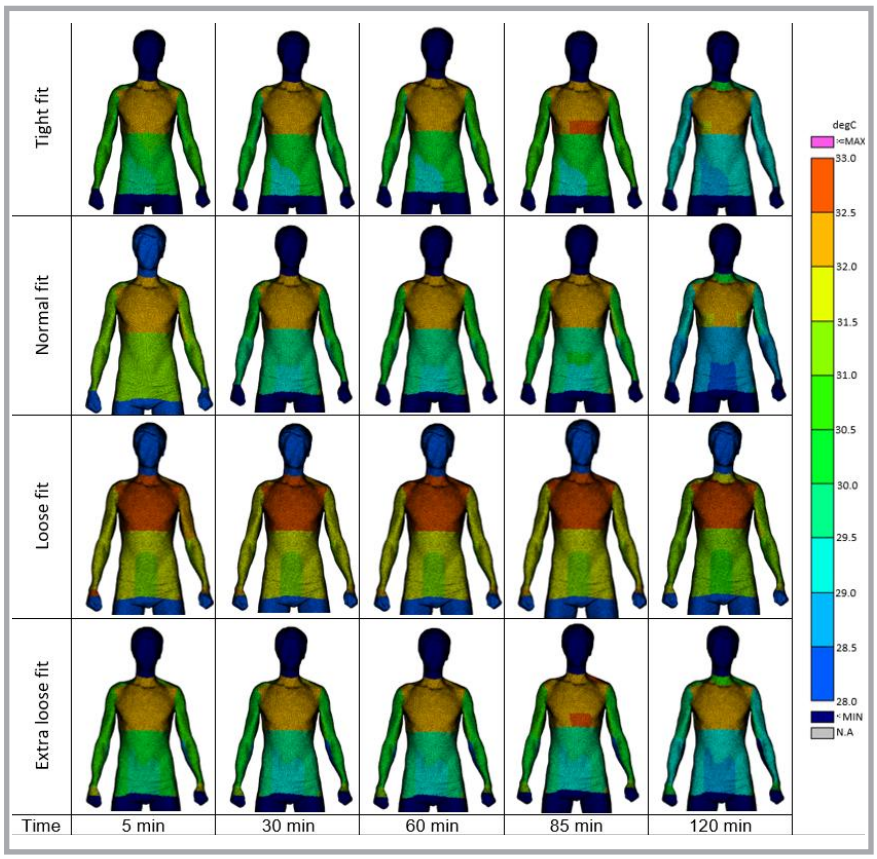

Figure 13. *Microclimate temperature at different time steps during thermal simulation.*

Acknowledgements

The authors would like to thank the AiF institution for providing funding for the IGF research project 19472 BG and express special thanks to ARRK Engineering GmbH for providing access to Theseus-FE software. Furthermore, the authors would like to specially acknowledge the Higher Education Commission, Govt. of the Pakistan and German Academic Exchange Service for its financial support of Dr. Muhammad Awais in his doctoral studies.

References

1. Parsons K. Human Thermal Environments [Internet]. Second. The Effects of Hot, Moderate, and Cold Environments on Human Health, Comfort and Performance. London and New York: Taylor and Francis Group; 2003. 1-538 p. Available from: http://onlinelibrary.wiley.com/doi/10.1002/cbdv.200490137/abstract
2. Lu Y, Song G, Li J. A Novel Approach for Fit Analysis of Thermal Protective Clothing Using Three-Dimensional Body Scanning. *Appl Ergon* [Internet]. 2014;45(6): 1439-46. Available from: http://dx.doi.org/10.1016/j.apergo.2014.04.007
3. McCullough EA, Jones BW. A Comprehensive Data Base for Estimating Clothing Insulation. *ASHRAE Trans*. 1984; 2888(2888): 29.
4. Havenith G, Heus R, Lotens Wa. Resultant Clothing Insulation: A Function of Body Movement, Posture, Wind, Clothing Fit and Ensemble Thickness. Ergonomics [Internet]. 1990 Jan 1;33(1):67-84. Available from: https://doi.org/10.1080/00140139008927094
5. Chen YS, Fan J, Qian X, Zhang W. Effect of Garment Fit on Thermal Insulation and Evaporative Resistance. Text Res J [Internet]. 2004 Aug 1;74(8):742-8. Available from: https://doi.org/10.1177/004051750407400814.
6. Daanen HAM, Hatcher K, Havenith G. Determination of clothing microclimate volume. In: 10th International Conference on Environmental Ergonomics [Internet]. Fukuoka, Japan; 2002. Available from: https://repository.lboro.ac.uk/articles/Determination_of_clothing_microclimate_volume/9339344.
7. Zhang Z, Li J. Volume of Air Gaps Under Clothing And Its Related Thermal Effects. J Fiber Bioeng Informatics [Internet]. 2011;4(2):137-44. Available from: http://global-sci.org/intro/article_detail/jfbi/4910.html.
8. Psikuta A, Frackiewicz-Kaczmarek J, Frydrych I, Rossi R. Quantitative Evaluation of Air Gap Thickness and Contact Area Between Body and Garment. *Text Res J*. 2012; 82(14): 1405-13.
9. Daanen HAM, Psikuta A. 10 – 3D body scanning. In: Nayak R, Padhye RBT-A in GM, editors. The Textile Institute Book Series [Internet]. United Kingdom: Woodhead Publishing; 2018. p. 237-52. Available from: http://www.sciencedirect.com/science/article/pii/B9780081012116000100.

10. Lee Y, Hong K, Hong SA. 3D Quantification of Microclimate Volume in Layered Clothing for the Prediction of Clothing Insulation. *Appl Ergon* 2007; 38(3): 349-55.
11. Frackiewicz-Kaczmarek J, Psikuta A, Bueno M. Effect of Garment Properties on Air Gap Thickness and the Contact Area Distribution. *Text Res J.* 2015; 85(18): 1907-18.
12. Mert E, Psikuta A, Arevalo M, Charbonnier C, Luible-Bär C, Bueno M-A, et al. Quantitative Validation of 3D Garment Simulation Software for Determination of Air Gap Thickness in Lower Body Garments Quantitative Validation of 3D Garment Simulation Software for Determination of Air Gap Thickness in Lower Body Garments. *In: AUTEX World Textile Conference 2017. Corfu, Greece.*
13. Awais M, Krzywinski S. Method Development for Modeling, Designing, and Digital Representation of Outdoor and Protective Clothing. *In: Majumdar A, Gupta D, Gupta S, editors. Functional Textiles and Clothing. Singapore: Springer Singapore*; 2019. p. 205-18.
14. Mert E, Psikuta A, Arévalo M, Charbonnier C, Luible-Bär C, Bueno M-A, et al. A Validation Methodology and Application of 3D Garment Simulation Software to Determine the Distribution of Air Layers in Garments During Walking. Measurement [Internet]. 2018;117:153-64. Available from: http://www.sciencedirect.com/science/article/pii/S0263224117307510.
15. Lotens WA, Havenith G. Calculation of Clothing Insulation and Vapour Resistance. Ergonomics [Internet]. 1991 Feb 1;34(2): 233-54. Available from: https://doi.org/10.1080/00140139108967309.
16. Li Y, Holcombe BV. Mathematical Simulation of Heat and Moisture Transfer in a Human-Clothing-Environment System. Text Res J [Internet]. 1998 Jun 1;68(6):389–97. Available from: https://doi.org/10.1177/004051759806800601.
17. Fan J, Luo Z, Li Y. Heat and Moisture Transfer with Sorption and Condensation in Porous Clothing Assemblies and Numerical Simulation. *Int J Heat Mass Transf* [Internet]. 2000; 43(16): 2989-3000. Available from: http://www.sciencedirect.com/science/article/pii/S0017931099002355.
18. Berger X, Sari H. A New Dynamic Clothing Model. Part 1: Heat and Mass Transfers. *Int J Therm Sci [Internet].* 2000; 39(6): 673-83. Available from: http://www.sciencedirect.com/science/article/pii/S1290072980002116.
19. Stolwijk JA, Nadel ER, Wenger CB, Roberts MF. Development and Application of a Mathematical Model of Human Thermoregulation. *Arch Sci Physiol* (Paris). 1973; 27(3): 303.
20. Fiala D, Lomas KJ, Stohrer M. A Computer Model of Human Thermoregulation for a Wide Range of Environmental Conditions: The Passive System. *J Appl Physiol* [Internet]. 1999 Nov 1; 87(5): 1957-72. Available from: https://doi.org/10.1152/jappl.1999.87.5.1957
21. Fiala D, Lomas KJ, Stohrer M. Computer Prediction of Human Thermoregulatory and Temperature Responses to a Wide Range of Environmental Conditions. *Int J Biometeorol* [Internet]. 2001; 45(3): 143-59. Available from: http://search.ebscohost.com/login.aspx?direct=true&db=cmedm&AN=11594634&site=ehost-live.
22. Tanabe S, Kobayashi K, Nakano J, Ozeki Y, Konishi M. Evaluation of Thermal Comfort Using Combined Multi-Node Thermoregulation (65MN) and Radiation Models and Computational Fluid Dynamics (CFD). Energy Build [Internet]. 2002; 34(6): 637-46. Available from: http://www.sciencedirect.com/science/article/pii/S0378778802000142.
23. Huizenga C, Hui Z, Arens E. A Model of Human Physiology and Comfort for Assessing Complex Thermal Environments. *Build Environ*. 2001; 36: 691-9.
24. Fanger P. Thermal Comfort : Analysis and Applications in Environmental Engineering. Danish Technical Press; 1970.
25. Fiala D, Lomas KJ, Stohrer M. First Principles Modeling of Thermal Sensation Responses in Steady-State and Transient Conditions. *ASHRAE Trans*. 2003; 109: 179.
26. Zhang H. Human Thermal Sensation and Comfort in Transient and Non-Uniform Thermal Environments. University of California, Berkley; 2003.
27. Fiala D, Havenith G, Bröde P, Kampmann B, Jendritzky G. UTCI-Fiala Multi-Node Model of Human Heat Transfer and Temperature Regulation. *Int J Biometeorol*. 2012; 56(3): 429-41.
28. Severens NMW, Lichtenbelt WD van M, Frijns AJH, Steenhoven AA Van, Mol BAJM de, Sessler DI. A Model to Predict Patient Temperature During Cardiac Surgery. Phys Med Biol [Internet]. 2007; 52(17): 5131-45. Available from: http://dx.doi.org/10.1088/0031-9155/52/17/002.
29. Psikuta A, Richards M, Fiala D. Single- and Multi-Sector Thermophysiological Human Simulators For Clothing Research. *In: 7th International Thermal Manikin and Modelling Meeting. Coimbra*; 2008. p. 1-5.
30. Fiala D, Lomas KJ. Application of a Computer Model Predicting Human Thermal Responses to the Design of Sports Stadia. *In: CIBSE '99, Conference Proc. Harrogate, UK*; p. 492-9.
31. Yang T, Cropper PC, Cook MJ, Yousaf R, Fiala D. A New Simulation System to Predict Human-Environment Thermal Interactions in Naturally Ventilated Buildings. *In: Proceedings of the 10th International Conference on Building Simulation* [Internet]. Beijing; 2007. p. 751-6. Available from: https://dspace.lboro.ac.uk/dspace-jspui/bitstream/2134/5255/1/BS2007_paper424.pdf.
32. Awais M, Krzywinski S, Wölfling B-M, Classen E. Thermal Simulation of Close-Fitting Sportswear. vol. 13, Energies. 2020.
33. Awais M, Krzywinski S, Wendt E. A Novel Modeling and Simulation Approach for the Prediction of Human Thermophysiological Comfort. *Text Res J* [Internet]. 2020 Sep 11;0040517520955227. Available from: https://doi.org/10.1177/0040517520955227.
34. Theseus FE [Internet]. [cited 2017 Oct 3]. Available from: http://www.theseusfe.com/simulation-software/human-thermal-model.
35. Paulke S. Finite Element Based Implementation of Fiala's Thermal Manikin in Theseus-FE [Internet]. 2007 [cited 2017 Aug 3]. Available from: http://www.theseus-fe.com/simulation-software/human-thermal-model.
36. Fiala D. Dynamic Simulation of Human Heat Transfer and Thermal Comfort (Thesis). Sustain Dev. 1998; 45(2001):1.
37. Pennes HH. Analysis of Tissue and Arterial Blood Temperatures in the Resting Human Forearm. *J Appl Physiol*. 1948; 1: 5-34.
38. Theseus-FE. Theory Manual 7.1.09. Munich, Germany; 2020.
39. Pandolf K, Givoni B, Goldman R. Predicting Energy Expenditure with Loads While Standing or Walking Very Slowly. *J Appl Physiol*. 1977; 43(4): 577-81.
40. Vitronic [Internet]. Available from: https://www.vitronic.com/industrial-and-logistics-automation/sectors/3d-body-scanner.html.
41. 3D scanning, design and reverse engineering software from 3D Systems Geomagic [Internet]. [cited 2016 Sep 7]. Available from: http://www.geomagic.com/en/.
42. GbR DKF. GRAFIS-Software [Internet]. [cited 2019 Aug 16]. Available from: https://www.grafis.com/files/Downloads/Infomaterial/Prospekt V12_EN_web.pdf.
43. Lectra [Internet]. [cited 2017 Jun 10]. Available from: http://www.lectra.com/en.
44. Incropera FP, DeWitt DP, Bergman TL, Lavine AS. Fundamentals of Heat and Mass Transfer [Internet]. SIXTH EDIT. US Patent 5,328,671. Chichester: John Willey & Sones; 2007. 997 p. Available from: http://www.google.com/patents?hl=en&lr=&vid=USPAT5328671&id=rb8lAAAAEBAJ&oi=fnd&dq=Heat+and+Mass+Transfer&printsec=abstract%5Cnhttp://www.google.com/patents?hl=en&lr=&vid=USPAT5328671&id=rb8lAAAAEBAJ&oi=fnd&dq=Heat+and+mass+transfer&printsec=abstract%5Cnh
45. Mert E, Psikuta A, Bueno MA, Rossi RM. Effect of heterogenous and homogenous air gaps on dry heat loss through the garment. *Int J Biometeorol*. 2015; 59(11): 1701-10.

Received 10.02.2021 Reviewed 12.05.2021


International Conference on
CELLULOSE FIBRES
2–3 February 2022


ICSTFD 2022: 16. International
Conference on Sustainable Textiles
and Fashion Design
July 19-20, 2022 in Paris, France


14th International Conference on Textile Composites
Kyoto Institute of Technology, Japan
14-16 September 2022


ICTDMMS 2022: 16. International Conference on Textile Development, Marketing
and Market Samples
August 30-31, 2022 in Rome, Italy
DIGITAL